

# Role of tunneling of hydrogen in the Norrish type II processes in a thione and a ketone

A.K. Chandra\*, V. Sreedhara Rao

Department of Inorganic and Physical Chemistry Indian Institute of Science, Bangalore 560 012, India

Received 5 December 1997; accepted 21 January 1998

## Abstract

Intra-molecular hydrogen abstraction reactions were examined in pentane-2-thione in its lowest triplet state using the AM-1 semiempirical molecular orbital method with the geometry optimisation in the unrestricted Hartree–Fock frame. Results were compared with those of pentane-2-one. The role of tunneling of hydrogen was examined in both the conventional transition-state approach and in the RRKM theory of unimolecular reactions. Results reveal that tunneling of hydrogen is less significant to sulfur than to oxygen. © 1998 Elsevier Science S.A. All rights reserved.

*Keywords:* Hydrogen tunneling; Thione; Ketone

## 1. Introduction

Ketones in their lowest triplet states [usually  $3(\eta\pi^*)$  states] abstract hydrogen by both intra- and inter-molecular photoelimination processes. Numerous experiments [1–3] and theoretical studies [4–9] reveal that a small barrier exists between the initially excited states of reactants and the primary reaction intermediates. From the temperature dependence of the rate constants and the deuterium isotope effect [10], one concludes that the nuclear tunneling is not important in the hydrogen-abstraction reactions. An observation of the very low value of this isotope effect may suggest that the primary step in the Norrish type II process is an electron-transfer rather than one-step hydrogen transfer. Although there is hardly any report of the isotope effect in the Norrish type II process, Grellmann et al. [11] and Al-Soufi et al. [12] reported a study on the photo enolisation process of 5:8 dimethyl 1-1 tetralone which revealed that the hydrogen transfer in this process is primarily controlled by tunneling around room temperatures. This process involves 1:5 hydrogen transfer on the lowest triplet state surface as in a Norrish type II process in a ketone. Recently, we [7,9] examined the role of tunneling of hydrogen in both the Norrish type II process and in the photo-enolisation process of a ketone [13]. We observed that in both cases, the tunneling of hydrogen is very significant around 300°K. There was no evidence of

operation of an electron-transfer mechanism [7,9] controlling the hydrogen-transfer process, even though the isotopic ratio  $K_H/K_D$  where  $K_H$  and  $K_D$  refer to the rate constants of the H- and D-transfer processes, respectively, is small at 300°K.

Scheffer [14] suggested that unless the abstractable hydrogen comes within 2.7–3.0 Å of the carbonyl oxygen, reaction cannot occur. This is made possible in pentane-2-one by an internal rotation around the  $\beta$ -bond relative to the carbonyl group. In our recent ab initio studies [9] of the Norrish type II process in pentane-2-one we observed that the barrier to rotation around the  $\beta$ -bond is negligible. In this paper, we study a thiocarbonyl compound analogous to pentane-2-one.

All thio carbonyl compounds show a long wavelength absorption band attributed to a  $\eta \rightarrow \pi^*$  transition [15,16]. Although not many reports are available on thio compounds, our report [17] on an inter-molecular reaction reveals that thione can abstract hydrogen at the position of sulfur by an in-plane process in its lowest  $\eta\pi^*$  state. de Mayo [18] reported that the intra-molecular reaction occurs at the  $\gamma$ -position relative to the thiocarbonyl group in the lowest triplet ( $\eta\pi^*$ ) state. However the life times of thiones are one to two orders of magnitude shorter than those of the corresponding ketones. This may be due to quenching of the excited state of thione by the ground state or the intersystem crossing efficiency in thione is close to unity [18]. In the absence of  $\gamma$ -hydrogen,  $\beta$ -abstraction has been observed.

\* Corresponding author.

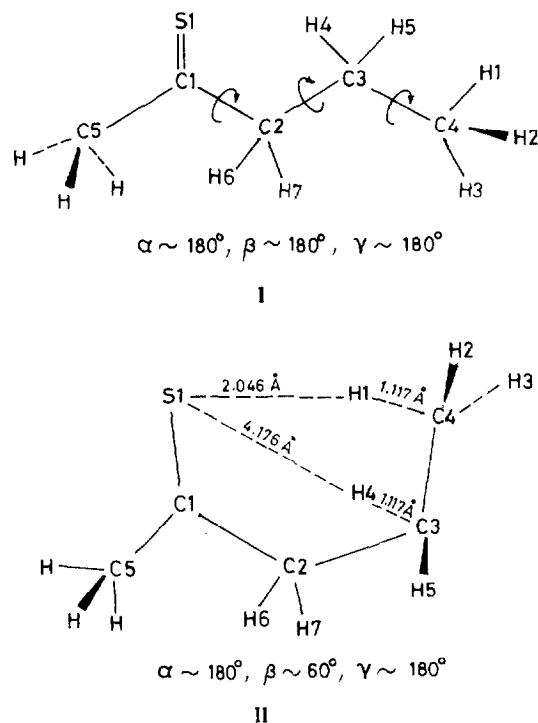


Fig. 1. Two conformers I and II of pentane-2-thione, each defined by the dihedral angles  $\alpha$ ,  $\beta$  and  $\gamma$ .

Fig. 1 shows the two conformers of pentane-2-thione defined by the dihedral angles  $\alpha$ ,  $\beta$  and  $\gamma$ . The conformer I is the equilibrium structure in the lowest triplet state. The conformer II is obtained by rotation around the  $\beta$ -bond where the S1...H1 distance is 2.046 Å and the S1...H4 distance, 4.176 Å. The structure II shows that while the  $\gamma$ -hydrogen abstraction should be easier, the  $\beta$ -hydrogen abstraction is possible in spite of the large S1-H4 distance, as the non-bonding 3p orbital on S is approximately double the size of the 2p nonbonding orbital of oxygen. No  $\beta$ -hydrogen abstraction is observed in a ketone. In this paper, we have undertaken an AM1 molecular orbital computational studies [19] of a thione (pentane-2-thione in Fig. 1) undergoing both intramolecular  $\gamma$ - and  $\beta$ -hydrogen abstractions in its lowest triplet state and examined the role of tunneling of hydrogen to sulfur in thione in the conventional transition state theory and in the RRKM theory of unimolecular reactions. We shall then make a comparative study of the relative rates of the Norrish type-II process in a ketone and a comparable thione maintaining the same level of calculations.

## 2. Computational method

We employed the AM1 method in the unrestricted Hartree-Fock (UHF) frame [19] and calculations were performed using the MOPAC program [20]. The UHF calculations allow different orbitals for each electron, which is preferable for treatment of the open-shell systems. Calculations were performed for various values of  $\alpha$ ,  $\beta$  and  $\gamma$  (Fig. 1) optim-

ising all the geometrical parameters. Since the intra-molecular hydrogen abstractions take place in the lowest triplet state, we examined the energetics of the conformational changes in the triplet state by the UHF/AM1 method. We consider two conformers I and II (Fig. 1) of the thione. The conformer II is energetically only 1.1 kJ/mol higher than the conformer I. We shall show that this energy is negligible compared to the activation barrier of the hydrogen-transfer reactions in the triplet state. Using the conformer II as reactant, we reduced the S1...H1 distance and the Broyden-Fletcher-Golfrab-Shanno optimisation procedure [20] was carried out until 1:4 biradical was obtained. A similar procedure was followed for the  $\beta$ -hydrogen abstraction reaction from the conformer II as reactant where the S1-H4 distance was reduced, until 1:3 biradical was obtained. These two biradicals were identified by the two highest singly occupied molecular orbitals localised on C1 and C4 in the case of 1:4 biradical and on C1 and C3 in the case of 1:3 biradical. In both cases, the transition state structures were characterised by only one negative eigen-value of the force constant matrix in each cases. The magnitude of the imaginary frequencies is  $1316i \text{ cm}^{-1}$  for the  $\gamma$ -hydrogen abstraction and  $1654i \text{ cm}^{-1}$  for the  $\beta$ -hydrogen abstraction reactions. It should be noted that the magnitude of the corresponding imaginary frequency in pentane-2-one is  $2148i \text{ cm}^{-1}$  [7]. The normal coordinate analysis shows that the eigenvector corresponding to the imaginary frequency is the asymmetric stretch of the non-linear triatomic systems S1-H1-C4 for the  $\gamma$ -hydrogen or S1-H4-C3 for the  $\beta$ -hydrogen abstraction reaction. We, therefore, chose the reaction coordinates  $X = R_{C4-H1} - R_{S1-H1}$  and  $X = R_{C3-H4} - R_{S1-H4}$  for the  $\gamma$ - and  $\beta$ -hydrogen abstraction reactions, respectively, where  $R_{Ci-Hj}$  and  $R_{Si-Hj}$  are respectively, the lengths of the  $Ci-Hj$  and  $Si-Hj$  bonds in thione. For the transition state structures and the reactant, all the real vibrational frequencies were calculated by a normal coordinate analysis on force constants derived analytically at the stationary points.

## 3. Results

Our calculations reveal that the 1:5 hydrogen transfer in the lowest triplet state of thione is endothermic by  $\sim 25 \text{ kJ/mol}$ , while the 1:4 hydrogen transfer process in the same thione is almost thermoneutral. The barriers for the hydrogen abstraction are nearly  $\sim 52 \text{ kJ/mol}$  for the  $\gamma$ -hydrogen abstraction and  $\sim 58 \text{ kJ/mol}$  for the  $\beta$ -hydrogen abstraction reactions, before the zero point vibrational energy (ZPVE) corrections. After the ZPVE corrections, the barrier heights are, respectively,  $35 \text{ kJ/mol}$  and  $\sim 40 \text{ kJ/mol}$ . For pentane-2-one the corresponding barrier height is  $\sim 44 \text{ kJ/mol}$  [7,9] while the reaction is exothermic, by  $65 \text{ kJ/mol}$  [7].

Fig. 2 shows the minimum energy paths (MEP) obtained by means of intrinsic reaction coordinate calculations for the intra-molecular  $\gamma$ - and  $\beta$ -hydrogen abstraction processes from the conformer II of the thione. For comparison, the MEP

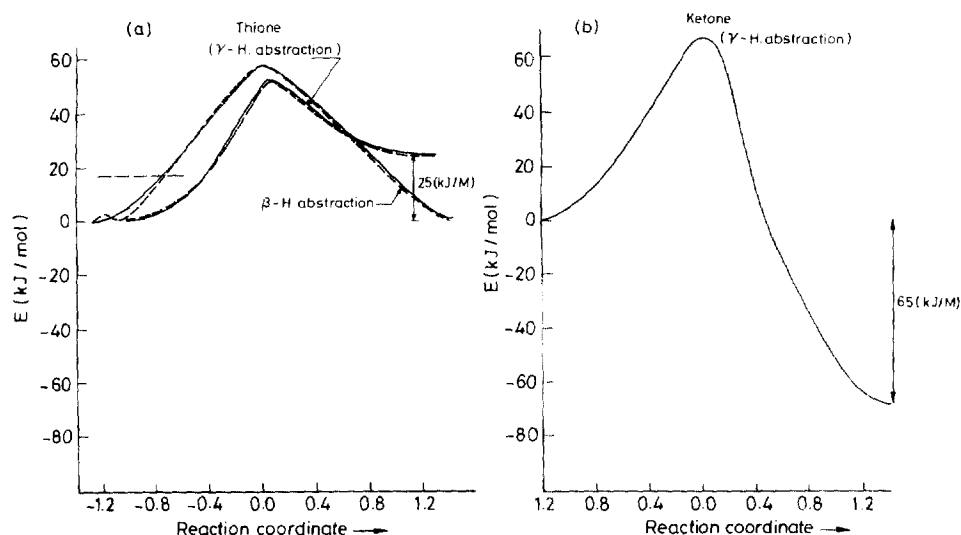


Fig. 2. (a) Minimum energy paths (MEP) for the  $\gamma$ - and  $\beta$ -hydrogen abstraction reactions in thione. (b) The corresponding MEP for the  $\gamma$ -hydrogen abstraction reaction in pentane-2-one. The solid lines are obtained by the AM1 (UHF) method, while the dashed lines in (a) refer to the fitted lines with the polynomial function of Eq. (2).

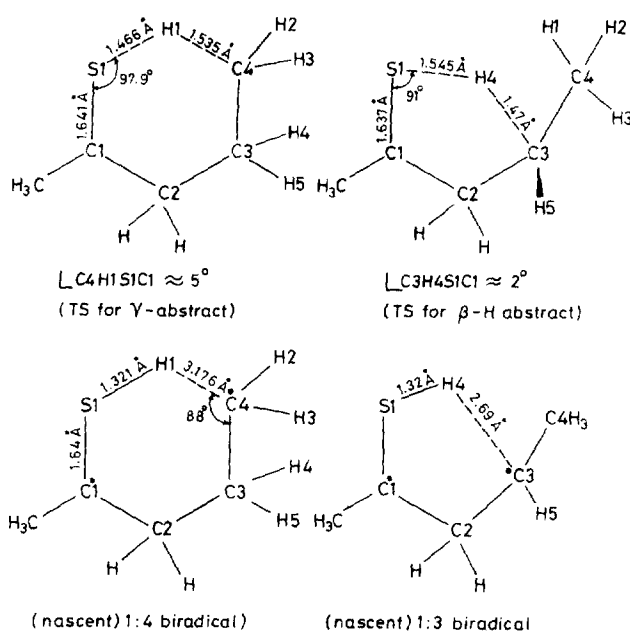


Fig. 3. The optimised structures of the transition-state (TS) and the nascent 1:4 and 1:3 biradicals. Bond lengths are given in angstroms.

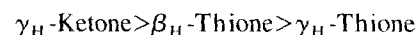
for the  $\gamma$ -hydrogen abstraction in pentane-2-one is also shown. Fig. 3 shows the optimised structures of the transition states for the  $\gamma$ - and  $\beta$ -hydrogen abstraction in thione and that of the 1:4 and 1:3 biradicals derived respectively from thione. For ketone the optimised structures were reported in our earlier papers [7,8].

#### 4. Discussion

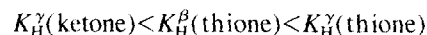
Intra-molecular hydrogen abstraction takes place in the lowest triplet state from the conformer II (Fig. 1) of thione as in pentane-2-one. The energy of the conformer II is only

1.1 kJ/mol higher than that of the conformer I. This energy is negligible compared to the activation barriers for the different hydrogen abstraction processes. The frequency of the internal rotation is  $\sim 10^{13} \text{ s}^{-1}$  which could be taken as the pre-exponential factor in a simple Arrhenius equation. This equation leads to an unimolecular rate constant of  $\sim 10^5 \text{ s}^{-1}$  at 300 K. No kinetic data are available for the reactions in thione but for pentane-2-one the rate constant of the  $\gamma$ -hydrogen abstraction in hexane has been measured and its value is  $2 \times 10^8 \text{ s}^{-1}$  at 300 K [21]. The observed larger rate constant for pentane-2-one has been attributed to a significant role of tunneling [7,9] of hydrogen even at 300 K.

Since the barrier heights for the different hydrogen transfer reactions decrease in the order



the Arrhenius rate constants should increase in the order.



where  $K_{\text{H}}$  refers to the unimolecular rate constant of the intra-molecular hydrogen transfer reaction, and the superscripts  $\gamma$  and  $\beta$  refer to the hydrogen abstraction from the  $\gamma$ - and  $\beta$ -positions of thione (or ketone), respectively.

#### 5. Structural properties of the transition states

The transition state structures for the  $\gamma$ - and  $\beta$ -hydrogen abstractions in pentane-2-thione are given in Fig. 3. The most important geometrical changes at the transition-state are the bond distances  $r^1$  and  $r$  of the newly forming S1–H1 and S1–H4 bonds and the breaking C4–H1 and C3–H4 bonds respectively, in the  $\gamma$ - and  $\beta$ -hydrogen transfer reactions. The relative bond distances  $r_{\text{rel}}^1$  and  $r_{\text{rel}}$  are defined as

$$r_{\text{rel}}^{\dagger} = \frac{r^{\dagger*}}{r_c^{\dagger}} \text{rel} = \frac{r^*}{r_c} \quad (1)$$

where  $r^{\dagger*}$  and  $r^*$  are the S1–H1 and C4–H1 bond distances in the transition-state and  $r_c^{\dagger}$  and  $r_c$  are the corresponding equilibrium bond-lengths in the product and the reactant, respectively from which H1 is abstracted. It has been shown [22] that the ratio  $r_{\text{rel}}^{\dagger}/r_c^{\dagger}$  is equal to unity for thermoneutral hydrogen transfer reactions, for the exothermic reactions this ratio is less than unity corresponding to more reactant like transition state and for the endothermic reactions this ratio should exceed unity corresponding to more product like transition-states. From the optimised bond length data shown in Fig. 3, we find that

$$\frac{\gamma_{\text{rel}}}{\gamma_{\text{rel}}^{\dagger}}$$

is 1.24 for the  $\gamma$ -hydrogen abstraction reaction in the thione. For the  $\beta$ -hydrogen transfer reaction which is approximately thermoneutral the ratio

$$\left( \frac{\gamma_{\text{rel}}}{\gamma_{\text{rel}}^{\dagger}} \right)$$

is around 1.12 instead of unity. It should be mentioned now that for the  $\gamma$ -hydrogen transfer reaction in pentane-2-one which is exothermic, this ratio

$$\frac{\gamma_{\text{rel}}}{\gamma_{\text{rel}}^{\dagger}}$$

was found to be 0.81 [7].

One would normally infer from reaction energetics that most exothermic channel usually has the lowest barrier. A closer examination of the structures of the transition states in thiones and ketone (Ref. [7]) indicates that the results obtained for the activation barriers are not consistent with expectation. The reactions that we compare here do not form a series for which simple structure–reactivity correlations apply. It is not surprising to note this, as the role of tunneling of hydrogen is very significant in intramolecular processes. The simple structure–reactivity correlations apply where tunneling is not significant.

## 6. Role of tunneling in the conventional transition state approach

Recently, we [13] reported studies on hydrogen tunneling in photoenolisation of a ketone and in the Norrish type II process of pentane-2-one [9]. Both processes involve 1:5 hydrogen transfer in their lowest triplet states. Our theoretical studies [7,9] along with the experimental works of Al Soufi et al. [12] reveal that tunneling is very significant in 1:5 hydrogen transfer processes from a C–H bond containing an abstractable hydrogen to oxygen. In this section, we consider tunneling of hydrogen to sulfur in intra-molecular processes.

Table 1

The barrier heights, energy of reactions, imaginary frequencies and barrier-widths of the potential surfaces of the  $\gamma$ - and  $\beta$ -hydrogen abstraction reactions

Reactions	Barrier height (kJ/mol)	$\Delta E^{\ddagger}$ (kJ/m)	Imaginary frequencies at the saddle point ( $\text{cm}^{-1}$ )	Barrier-width (Å)
1. $\gamma$ -H abstraction in ketone	44	–65	2148i $\text{cm}^{-1}$	0.9
2. $\gamma$ -H abstraction in thione	35	(+25)	1317i $\text{cm}^{-1}$	1.2
3. $\beta$ -H abstraction in thione	40	0.0	1654i $\text{cm}^{-1}$	1.4

<sup>†</sup>  $\Delta E$  stands for reaction energy.

Table 1 shows the imaginary frequencies at the saddle points for both  $\gamma$ - and  $\beta$ -hydrogen transfer reactions in thione. For comparison, the imaginary frequency observed for pentane-2-one is also given [7]. The imaginary frequency measures the curvature at the saddle point, in other words the width of the barrier. Higher the imaginary frequency at the saddle point, lower is the width of the barrier and more significant is the role of tunneling of hydrogen. To determine the role of tunneling in the intramolecular  $\beta$ - and  $\gamma$ -hydrogen abstraction processes in thione we follow the same procedure as described in our earlier papers [7,9].

To calculate the probability of tunneling we fit the theoretically calculated MEP with the following polynomial function.

$$V(x-x_0) = V_0 + \sum_{i=1}^7 li(x-x_0)^i \quad (2)$$

where  $x_0$  is the value of the reaction coordinate at the transition state and  $V_0$  is the energy barrier for the reaction. The coefficients  $li$  in Eq. (1) are constants with appropriate dimensions. The above seventh order polynomial fits well with the theoretically computed one-dimensional energy profiles for both thione and ketone.

For calculation of the probability,  $P(E)$  of hydrogen tunneling, we use the WKB method of approximation [23].  $P(E)$  is given by

$$P(E) = \exp \left[ -2 \left( \frac{8\pi^2\mu}{h^2} \right) \int_{a(E)}^{b(E)} |V(x) - E|^{1/2} dx \right] \quad (3)$$

where  $V(x)$  is the potential function given by Eq. (2) above,  $E$  is the energy of the tunneling particle,  $\mu$  is the reduced mass,  $b(E) - a(E)$  is the tunneling distance which depends on  $E$  according to Fig. 2 and  $h$  is Planck's constant. The integral in Eq. (3) is evaluated by numerical integration. The specific unimolecular rate constant  $K(E)$  for the hydrogen transfer processes may be given by the product of the fre-

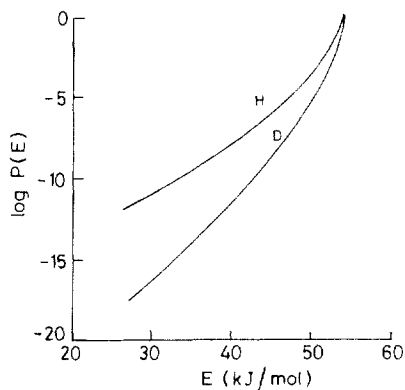


Fig. 4. The plots of  $\log P(E)$  vs.  $E$  (in kJ/mol) for the  $\gamma$ -hydrogen and  $\gamma$ -deuterium abstraction processes in pentane-2-thione for the  $\gamma$ -hydrogen abstraction process.

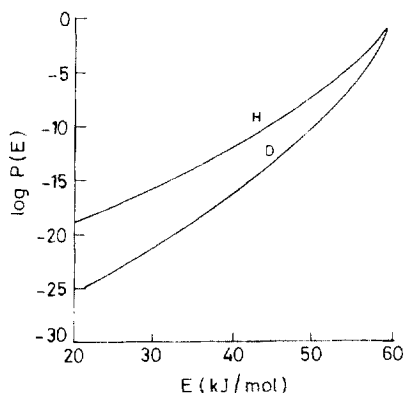


Fig. 5. The plots of  $\log P(E)$  vs.  $E$  (in kJ/mol) for the hydrogen and deuterium substituted pentane-2-thione for the  $\beta$ -hydrogen abstraction process.

quency factor  $\gamma_{\text{eff}}$  where  $\gamma_{\text{eff}}$  is the effective frequency and the barrier permeability  $P(E)$ , i.e.,  $K(E) = \gamma_{\text{eff}} P(E)$ . The frequency factor  $\gamma_{\text{eff}}$  involves the stretching of the C–H bond and the bending motion of the H1–C4–C3 in thione. The two harmonic degrees of freedom have been converted into one effective degree of freedom with frequency  $\gamma_{\text{eff}}$  as outlined in previous papers [7,9]. The effective frequencies  $\gamma_{\text{eff}}^{\text{H}}$  and  $\gamma_{\text{eff}}^{\text{D}}$  for the  $\gamma$ -hydrogen transfer process in thione calculated from the AM-1 frequencies are  $2540 \text{ cm}^{-1}$  and  $1860 \text{ cm}^{-1}$ , respectively. For  $\beta$ -hydrogen transfer processes  $\gamma_{\text{eff}}^{\text{H}}$  and  $\gamma_{\text{eff}}^{\text{D}}$  are nearly same as those for the corresponding  $\gamma$ -hydrogen transfer reactions.

Figs. 4 and 5 show the variation of  $\log P(E)$  with  $E$  for hydrogen and deuterium tunneling during the  $\gamma$ - and  $\beta$ -hydrogen abstraction processes, respectively, in thione. The  $\gamma$ -hydrogen abstraction process is endothermic. After the ZPVE corrections of the reactant, transition state and 1:4 biradical (product), we find that the lowest vibrational level of the product lies  $\sim 10 \text{ kJ/mol}$  above the lowest level of the reactant. The tunneling of hydrogen in the  $\gamma$ -hydrogen transfer reaction is therefore, forbidden until the energy of the reactant lies  $10 \text{ kJ/mol}$  above the lowest vibrational level of the reactant. Since weaker the C–H bond, higher is the position of the minimum of its potential well as both strong and weak

C–H bonds dissociate into the same limit, the tunneling probability will increase from the weaker C–H bonds to sulfur in thione. This has been shown in both intra- [24] and intermolecular [25] processes. On the other hand, the hydrogen abstraction from the  $\beta$ -position in thione is almost thermo-neutral.

Both Figs. 4 and 5 show that there is a finite probability of tunneling of both hydrogen and deuterium when  $E$  is smaller than the barrier height. And as the energy increases the probability of deuterium tunneling increases at a faster rate and both converge to a value close to unity when the total energy reaches  $\sim 60 \text{ kJ/mol}$  (approx.) relative to ZPVE of the reactant.

We then take a thermal average of the specific rate constant at a given temperature,  $T$ . It is known that the temperature-dependence of tunneling rate constant is caused by thermally activated tunneling. To describe the transition from temperature-dependent to temperature-independent tunneling, one should take into account low frequency vibrational as well as rotational modes as outlined in our earlier papers [7,9]. We observed nine low-frequency modes in the range  $30 \sim 450 \text{ cm}^{-1}$  for thione in its lowest triplet state. The thermally averaged rate constant at a given temperature,  $T$ , is given by

$$K(T) = \gamma_{\text{eff}} X \frac{\sum_{i_1, i_2} \dots \sum_{i_n} \dots \sum_{j_1} \dots \sum_{j_3} P(E_{v_r}) \exp\left(-\frac{E_{v_r}}{K_b T}\right)}{\sum_{i_1, i_2} \dots \sum_{i_n} \dots \sum_{j_1} \dots \sum_{j_3} \exp\left(-\frac{E_{v_r}}{K_b T}\right)} \quad (4)$$

where  $i$  and  $j$  are the low frequency vibrational and three rotational modes respectively.  $K_b$  is the Boltzmann constant, and  $E_{v_r}$  is the rotational–vibrational energy of the reactant.  $E_{v_r}$  is given by

$$E_{v_r} = E_{\text{ZPVE}} + v_1 h\nu_1 + v_2 h\nu_2 + \dots + \sum_{i=1}^{i=3} j_i(j_i+1)B_i \quad (5)$$

where  $E_{\text{ZPVE}}$  is the total zero-point energy of thione.  $B_i$ s are its rotational constants. Since  $E_{v_r}$  consists of rotational as well as low frequency vibrational modes, it will be a reasonable approximation to replace the summation by integration. Hence, we write Eq. (4) as

$$K(T) = \gamma_{\text{eff}} \frac{\int_{\text{ZPVE}}^{\infty} N(E_{v_r}^1) P(E_{v_r}^1) \exp\left(-\frac{E_{v_r}^1}{K_b T}\right) dE}{\int_{\text{ZPVE}}^{\infty} N(E_{v_r}^1) \exp\left(-\frac{E_{v_r}^1}{K_b T}\right) dE} \quad (6)$$

where  $E_{v_r}^1 = E_{v_r} - E_{\text{ZPVE}}$ , and  $N(E_{v_r}^1)$  is the density of states of the reactant at a non-fixed energy  $E_{v_r}^1$  which has been calculated using the Whitten–Rabinovitch approximation [26] for nine low frequency vibrational modes. Our results show that  $N(E_{v_r}^1)$  increases with energy considerably and then flattens off at higher energies, as shown earlier for a

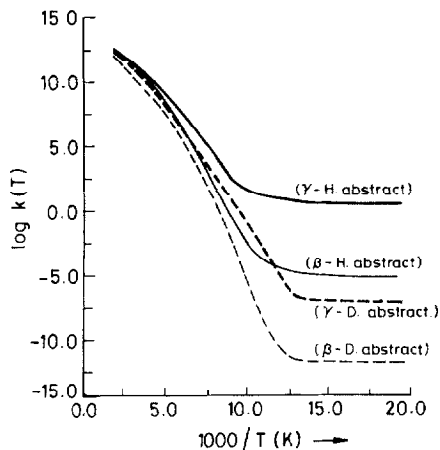


Fig. 6. The plots of  $\log K_H$  (or  $\log K_D$ ) vs.  $1000/T$ . The solid lines refer to H-transfer and the dashed lines refer to D-transfer in thione.

ketone [9]. The density of states is always higher when the migrating hydrogen is substituted for deuterium.

The plots of  $\log K_H(K_D)$  vs.  $1000/T$  are shown for  $\gamma$ -hydrogen and  $\beta$ -positions in thione in Fig. 6. Results reveal that below 77 K the rate constants of the hydrogen and deuterium abstractions from the  $\gamma$ - and  $\beta$ -positions in thione become almost temperature-independent and are too slow to compete with the intersystem crossing which has been observed in ketone to be almost temperature-independent and isotope-independent [12]. Fig. 6 shows that both H- and D-transfer rate constants decrease rapidly in thione with decreasing temperature at very low temperature. It is unlikely to observe the H-transfer process at low temperatures as the intersystem crossing to the ground state may dominate. Besides, the lower energy gap [15,16] between the lowest triplet state and ground state in thione than in ketone makes thione more photostable than ketone, owing to more efficient intersystem crossing in thione. The calculated isotopic ratio, i.e.,  $K_H/K_D$  for the  $\gamma$ -hydrogen abstraction process is 2.5 while for the  $\beta$ -hydrogen abstraction process is 6.0 in thione at 300 K. The calculated ratio  $K_H/K_D$  for pentane-2-one is 7 at 300 K [7]. Theoretically, the small isotope effect is expected in both thione and ketone but this does not mean that an electron-transfer mechanism operates. The tunneling factors,  $[H]$  are always high in both ketone and thione. For example, at 300 K, the tunneling factors  $[H]^\gamma$  and  $[H]^\beta$  in thione are  $0.28 \times 10^3$  and  $0.18 \times 10^3$  while  $[D]^\gamma$  and  $[D]^\beta$  are  $0.15 \times 10^3$  and  $0.42 \times 10^3$ , respectively. This leads to a ratio of  $[H]^\gamma/[D]^\gamma$  and  $[H]^\beta/[D]^\beta$  of 2 and 4, respectively, while for ketone  $[H]^\gamma/[D]^\gamma$  is 0.03 at 300 K. Thus, in ketone the deuterium tunneling dominates the hydrogen tunneling while in thione hydrogen tunneling always dominates.

At high temperatures, both the H- and D-transfer rate constants converge nearly to the same value, as in pentane-2-one. But if we compare the tunneling factors of a ketone with that of a comparable thione, we always find that the tunneling factor of ketone is higher than that in thione. Fig. 7 shows the plots of  $[H]^\gamma(K)/[H]^\beta(T)$  and  $[H]^\gamma(K)/[H]^\gamma(T)$  against temperature  $T$ , where K and T within brackets refer to ketone and

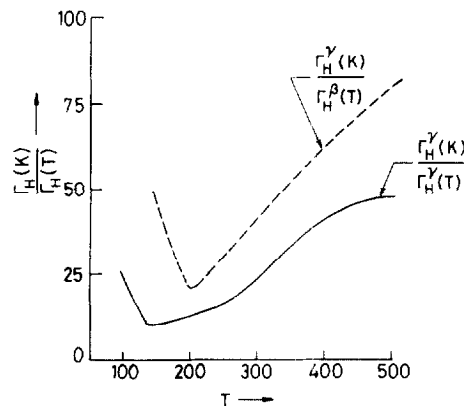


Fig. 7. The plots of  $[H](K)/[H](T)$  against  $T$  where K and T within brackets refer to ketone and thione, respectively, the superscripts  $\gamma$  and  $\beta$  refer to abstraction from the  $\gamma$ - and  $\beta$ -positions relative to the thiocarbonyl or carbonyl group.

thione, respectively. This figure indicates that tunneling of hydrogen to oxygen in a ketone is more significant than to sulfur in a comparable thione, in the temperature-range of 100 ~ 500 K. At lower than 100 K, the tunneling ratios are anomalously large. One can also observe that tunneling of hydrogen from the  $\gamma$ -position is higher than that from the  $\beta$ -position to sulfur in thione.

## 7. Tunneling corrections to the RRKM theory

Tunneling corrections [27] to the rate constant for unimolecular reactions can be treated within the RRKM theory [28] of the  $\gamma$ -hydrogen abstraction reactions of a ketone and a comparable thione. A simple way to include the effect of tunneling is to assume that the one-dimensional motion along the reaction coordinate is separable from the other degrees of freedom. The expression for the unimolecular rate constant which incorporates tunneling is given by [27]

$$K_{QM}(E_v) = \frac{P(E_v)}{2\pi N_0(E_v)} \quad (7)$$

$$N_0'(E_v) = \frac{\partial N_0(E_v)}{\partial E} \quad (8)$$

where  $E_v$  is the vibrational energy for the nine low frequency vibrational modes of the reactant (ketone or thione) relative to the total zero point vibrational energy of the reactant.  $P(E_v)$  is the probability of tunneling calculated by the numerical integration of Eq. (3) for the different values of  $E_v$ .  $N_0(E_v)$  is the integral densities of states for the reactant molecule which have been computed using the Whitten–Rabinovich approximation [26]. The simple classical rate constant is given by [28]

$$K(E) = A \left( \frac{E - V_0}{E} \right)^{s-1} \quad (9)$$

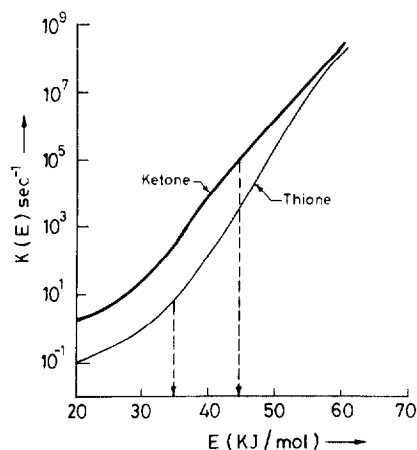


Fig. 8. The plots of  $\log K(E)$  vs.  $E$  (kJ/mol). The thick and thin lines refer respectively to ketone and thione. The vertical broken lines refer to the classical rate constants, which vanish when  $E < V_0$ .

$$A = \frac{\prod_i^S (\nu_i)}{\prod_i^{S-1} (\nu_i^*)} \quad (10)$$

where  $S$  is the number of vibrational degrees of freedom of the reactant,  $\{\nu_i\}$  and  $\{\nu_i^*\}$  are the normal mode frequencies of the reactant and transition state and  $V_0$  is the bare barrier height plus the zero-point energy of the transition state, i.e., the energy of the saddle point of the potential energy surface relative to the total zero point vibrational energy of the reactant. The classical rate constant vanishes when  $E < V_0$ . Our calculations reveal that the density of reactant states, i.e.,  $N_0(E_v)$  and the probabilities  $P(E_v)$  of tunneling using Eq. (3) are higher in thione than in the comparable ketone (pentane-2-one) for any given energy  $E_v$ . While the density of states in thione are two order of magnitude higher than that in ketone, the tunneling probabilities are only slightly higher in thione owing to its larger barrier-width. Therefore, the overall unimolecular rate constant is always higher in ketone than in the corresponding thione. These are relative rate constants and do not refer to their absolute values. Fig. 8 shows the unimolecular rate constant  $K(E)$  as function of energy  $E$ , relative to the total ZPE of the reactant for the  $\gamma$ -hydrogen abstraction process in ketone and in the comparable thione. Calculations were carried out for the total angular momentum  $J=0$ . For comparison the classical rate constants are shown by the vertical broken lines which show the positions of the barriers on the energy axis. Below this threshold energy the classical rate constant is zero. One sees that tunneling of hydrogen allows a significant rate constant ( $\sim 10^5 \text{ s}^{-1}$ ) to ketone at its threshold energy while the unimolecular rate constant of thione is only  $10^{+1} \text{ s}^{-1}$  at the corresponding threshold energy. This shows that tunneling plays a more significant role in ketone than in thione even though the bare barrier height for ketone is higher than that in thione.

## 8. Conclusions

We conclude that photochemical intra-molecular  $\gamma$ -hydrogen abstraction in a ketone and a comparable thione occur

via tunneling of hydrogen at high temperatures while their isotopic ratios are small. The tunneling of hydrogen is more significant to oxygen in a ketone than to sulfur in a thione. This is consistent with the larger barrier-width and lower imaginary frequencies for thione than those for ketone. The sulfur atom of thione can also abstract hydrogen, less readily, from the  $\beta$ -position as this reaction has a slightly large barrier height and barrier-width relative to that from the  $\gamma$ -position. A similar intra-molecular  $\beta$ -hydrogen abstraction process is not observed in a ketone.

## Acknowledgements

One of the authors (A.K.C.) thanks the CSIR (Govt. of India) for financial support.

## References

- [1] N.J. Turro, Modern Molecular Photochemistry, Chaps. 8, 10. The Benjamin Cummings Publishing, Menlo Park, CA, USA (1978).
- [2] N.C. Yang, D.H. Yang, J. Am. Chem. Soc. 80 (1958) 2931.
- [3] P.J. Wagner, Acc. Chem. Res. 4 (1971) 168.
- [4] D. Sengupta, R. Sumathy, A.K. Chandra, J. Photochem. Photobiol. A: Chem. 60 (1991) 149.
- [5] D. Sengupta, A.K. Chandra, J. Photochem. Photobiol. A: Chem. 73 (1993) 151.
- [6] D. Sengupta, A. Bhattacharya, R. Sumathy, A.K. Chandra, J. Photochem. Photobiol. A: Chem. 86 (1995) 161.
- [7] V. Sreedhara Rao, A.K. Chandra, J. Photochem. Photobiol. A: Chem. 101 (1996) 189.
- [8] A.E. Dorigo, M.A. McCarrick, R.J. Lonchariach, K.N. Houk, J. Am. Chem. Soc. 112 (1990) 7508.
- [9] V. Sreedhara Rao, A.K. Chandra, Chem. Phys. 214 (1997) 103.
- [10] P. Suppan, J. Chem. Soc. Faraday Trans. 2 (1986) 82.
- [11] K.H. Grellmann, H. Weller, E. Taur, Chem. Phys. Lett. 95 (1983) 195.
- [12] W. Al-Soufi, E. Eychmaller, K.H. Grellmann, J. Phys. Chem. 95 (1991) 2022.
- [13] D. Sengupta, A.K. Chandra, Int. J. Quantum Chem. 52 (1994) 1317.
- [14] J.R. Scheffer, Org. Photochem. 8 (1987) 249.
- [15] D.S.L. Blackwell, C.C. Liao, R.O. Loutfy, P. de Mayo, S. Paszyc, Mol. Photochem. 4 (1972) 171.
- [16] G.N. Lewis, M. Kasha, J. Am. Chem. Soc. 67 (1945) 994.
- [17] K. Sumathi, A.K. Chandra, J. Photochem. Photobiol. A: Chem. 43 (1988) 313.
- [18] P. de Mayo, Acc. Chem. Res. 9 (1976) 52.
- [19] M.J.S. Dewar, E.G. Zoebish, E.F. Healy, J.J.P. Stewart, J. Am. Chem. Soc. 107 (1985) 3902.
- [20] M.J.S. Dewar, E.G. Zoebish, E.F. Healy, J.J.P. Stewart, Quantum Chemistry Exchange Package No. 455 (1985).
- [21] P.J. Wagner, G.S. Hammond, J. Am. Chem. Soc. 88 (1966) 1245.
- [22] R. Daudel, C. Leroy, D. Peters, M. Sana, Quantum Chemistry, Chap. 6, Wiley, New York (1983).
- [23] D. Park, Introduction to Quantum Theory, McGraw-Hill, New York, USA (1974).
- [24] P. de Mayo, R. Suau, J. Am. Chem. Soc. 96 (1974) 6807.
- [25] A. Ohno, N. Kito, Int. J. Sulfur Chem., Part A 1 (1971) 26.
- [26] G.Z. Whitten, B.S. Rabinovitch, J. Chem. Phys. 38 (1963) 2466.
- [27] W.H. Miller, J. Am. Chem. Soc. 101 (1979) 6810.
- [28] P.J. Robinson, K.A. Holbrook, Unimolecular Reactions, Wiley, New York (1972).